

Aerial Vision-Language Navigation with a Unified Framework for Spatial, Temporal and Embodied Reasoning

Huilin Xu, *Graduate Student Member, IEEE*, Zhuoyang Liu, *Graduate Student Member, IEEE*,
Yixiang Luomei, *Member, IEEE*, and Feng Xu, *Senior Member, IEEE*

Abstract—Aerial Vision-and-Language Navigation (VLN) aims to enable unmanned aerial vehicles (UAVs) to interpret natural language instructions and navigate complex urban environments using onboard visual observation. This task holds promise for real-world applications such as low-altitude inspection, search-and-rescue, and autonomous aerial delivery. Existing methods often rely on panoramic images, depth inputs, or odometry to support spatial reasoning and action planning. These requirements increase system cost and integration complexity, thus hindering practical deployment for lightweight UAVs. We present a unified aerial VLN framework that operates solely on egocentric monocular RGB observations and natural language instructions. The model formulates navigation as a next-token prediction problem, jointly optimizing spatial perception, trajectory reasoning, and action prediction through prompt-guided multi-task learning. Moreover, we propose a keyframe selection strategy to reduce visual redundancy by retaining semantically informative frames, along with an action merging and label reweighting mechanism that mitigates long-tailed supervision imbalance and facilitates stable multi-task co-training. Extensive experiments on the Aerial VLN benchmark validate the effectiveness of our method. Under the challenging monocular RGB-only setting, our model achieves strong results across both seen and unseen environments. It significantly outperforms existing RGB-only baselines and narrows the performance gap with state-of-the-art panoramic RGB-D counterparts. Comprehensive ablation studies further demonstrate the contribution of our task design and architectural choices.

Index Terms—unmanned aerial vehicle (UAV), aerial navigation, Vision-and-Language Navigation (VLN)

I. INTRODUCTION

UNMANNED Aerial Vehicle (UAV) has become an indispensable tool in modern remote sensing applications, playing a central role in infrastructure inspection, environmental monitoring, and emergency response [1], [2]. Previous research has largely focused on passive perception tasks, including object detection [3], [4] and tracking [5], [6] from aerial images or videos, without interaction with the world. In contrast, aerial navigation tasks require the drone to perceive, reason, and act in dynamic environments. Recently, aerial Vision-and-Language Navigation (VLN) [7] has emerged as a new paradigm, where drones follow high-level language instructions to navigate the destination through 3D outdoor environments. By leveraging natural language as a human-centric interface, aerial VLN significantly reduces the reliance on expert pilots, lowers the barrier of human-UAV interaction,

The authors are with the Key Laboratory for Information Science of Electromagnetic Waves (Ministry of Education), School of Information Science and Technology, Fudan University, Shanghai 200433, China (e-mail: fengxu@fudan.edu.cn).

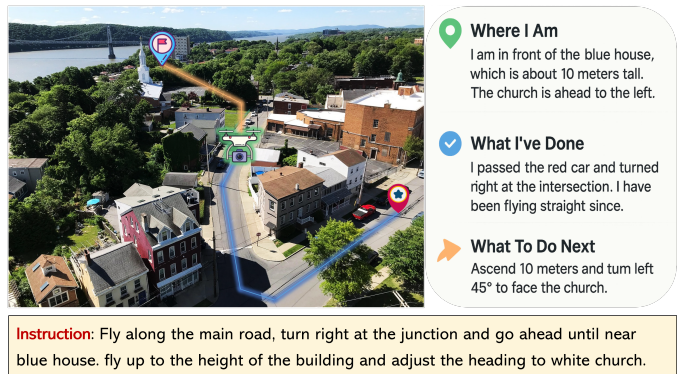


Fig. 1. Aerial vision-language navigation. Left: A drone receives a natural-language instruction along with egocentric visual observations and is required to navigate to the destination in a complex outdoor environment. Right: This task relies on the agent's ability to maintain an accurate understanding of its navigational situation, including estimating its current position, interpreting its progress within the instruction, and determining the next movement consistent with the described route. The example highlights these dimensions of temporal and spatial reasoning, which are central to reliable long-horizon aerial navigation.

and enables intuitive task specification in high-stakes scenarios.

Recent works have explored the design of benchmarks and datasets to facilitate research in aerial vision-and-language navigation. AVDN [8] first proposed a dialogue-based setting involving asynchronous interactions between a human commander and a UAV agent. AerialVNL [7] introduced high-fidelity city-scale simulations with diverse human-annotated trajectories. CityNav [9] extended this line by leveraging real-world urban reconstructions. OpenUAV [10] formulated aerial VLN as full-trajectory prediction with human-in-the-loop evaluation, and OpenFly [11] scaled up scene and instruction diversity via automatic generation. AeroDuo [12] explores the collaborative setting with multi-agent instruction following with altitude-aware role assignment. Moreover, CityEQA [13] and 3D Open-EQA [14] have proposed embodied question answering benchmarks to assess model's perception and reasoning capabilities from aerial perspective. However, as illustrated in Fig. 1, aerial VLN requires an agent to continuously integrate current observation, trajectory history, and high-level instruction. Concretely, the agent must recognize location from egocentric views, assess task progress relative to instruction, and infer the next action consistent with the intended route. Aerial VLN presents unique challenges across three core aspects.

1) *Unified Vision-Language-Action Alignment*: UAVs strug-

gle for high-dimensional action spaces involving both horizontal and vertical movements, where altitude changes affect visibility, orientation, and control feasibility. Mapping free-form natural language instructions to executable flight commands requires reliable alignment between egocentric semantics and spatial geometry.

- 2) *Large-scale Outdoor Aerial Scenes*: UAVs operate in large-scale urban environments with dense infrastructures, complex spatial layouts, and highly dynamic semantic distributions. This complexity demands precise spatial perception (*"ascend to the height of the street lamp"*) and the ability to robustly ground language-referred landmarks (*"the gray house with a slope"*) using egocentric observations.
- 3) *Long-Horizon Temporal Reasoning*: Aerial instructions often describe multi-stage flight plans that span long distances and evolving visual contexts. Agents must not only interpret sequential goals but also maintain trajectory-level awareness, track historical behavior, and align current decisions with global navigation intent.

Massive endeavors have attempted to alleviate these challenges. A line of work methods leverages pre-trained vision-language models (VLMs) to enable zero-shot instruction following. STMR [15] encodes current egocentric view, drone pose, and subgoal cues into a matrix-form prompt, allowing the language model to reason over spatial structures and landmarks. CityNavAgent [16] enhances semantic grounding by constructing symbolic 2D landmark maps from real aerial imagery combined with object detection. In contrast, other line of work aims to directly align visual observations with language instructions through joint training. LAG [7] combines a look-ahead guidance mechanism to Cross-Modal Attention method [17]. CityNav [9] introduces geographic semantic map (GSM), which integrates map data retrieved from OpenStreetMap with the pose of drones. Grid-based View Selection [18] reformulates the navigation task as a coupled horizontal–vertical view selection problem, integrating bird’s-eye fusion and cross-modal alignment. While these approaches have achieved promising performance, many of them rely on auxiliary inputs such as panoramic cameras, depth sensors, odometry or maps. These modalities lead to significant hardware cost and complexity. These design choices hinder generalizability and make them less suitable for real-world UAV deployment.

In this paper, we aim to develop a unified framework for aerial VLN, which relies solely on onboard egocentric RGB observations and natural language instructions. Without the need of any panoramic images, depth information, odometry and maps, our method directly predicts the next action step-by-step, bridging language semantics with visual context. Under the Next-Token Prediction (NTP) paradigm, we jointly models spatial perception, trajectory reasoning, and high-level action prediction within a single vision-language backbone. Task-specific prompts are introduced to steer learning towards distinct reasoning objectives while preserving architectural elegance and training efficiency. To mitigate redundancy in long-horizon video trajectories, we adopt an egocentric keyframe

selection mechanism that retains informative frames and significantly reduces the computational burden caused by massive visual tokens. Furthermore, we design an action-merge and label reweighting strategy to alleviate label imbalance and facilitate multi-task co-training. All tasks are co-optimized under a unified vision-language interface, encouraging the model to satisfy the nature of aerial VLN, which demands precise spatial grounding, temporal abstraction, and embodied control. Experimental results demonstrate that our method consistently outperforms baseline models. Our contributions can be summarized as follows:

- 1) We develop an egocentric aerial VLN framework that relies solely on monocular front-view RGB observations and natural language instructions, removing the need for panoramic inputs, depth sensors, odometry, or pre-built maps. The proposed model directly maps textual instructions and egocentric visual observations into executable navigation actions.
- 2) We formulate aerial VLN as a unified next-token prediction problem, where spatial perception, trajectory reasoning, and action generation are jointly optimized under a unified vision-language interface via task-specific prompts. Moreover, we proposed a keyframe selection strategy to reduce visual redundancy, along with an action-merge and label reweighting mechanism to mitigate label imbalance.
- 3) We conduct extensive experiments on standard benchmarks, achieving state-of-the-art performance and validating the effectiveness of each proposed component through comprehensive ablation studies.

II. RELATED WORKS

A. Aerial Navigation

Aerial navigation has attracted growing attention, with early efforts focusing on conventional tasks such as obstacle avoidance [19], [20] and object tracking [21], [22] based on onboard cameras or GPS signals. Recent advances explore language-guided aerial navigation, aiming to empower UAVs to interpret and execute natural language instructions in large-scale, open-world scenarios [7]. This task introduces additional challenges beyond visual navigation, such as grounding language instructions into visual perception and continuous control, performing temporal reasoning, and aligning multimodal information for robust decision-making. AVDN [8] introduces a dialogue-based UAV-VLN setting with asynchronous commander–follower interactions. AerialVNL [7] collects diverse human-piloted trajectories paired with spatially grounded instructions in synthetic outdoor cities, while CityNav [9] leverages real-world 3D urban reconstruction. OpenUAV [10] formulates UAV-VLN as full-trajectory prediction and incorporates human-in-the-loop evaluation. OpenFly [11] scales up dataset diversity through automatic generation over varied high-fidelity virtual environments.

Early approaches to aerial VLN adapted models from ground-based navigation but often struggled with dynamic viewpoints and large-scale outdoor complexity. More recently,

with the rise of large language models (LLMs) and vision language models (VLMs), several works have explored training-free paradigms that exploit their visual reasoning and visual grounding abilities for zero-shot aerial VLN [23]–[25]. The line for this work converts visual observations into text prompts, in the form of topological graphs, symbolic maps, or structured semantic matrices and rely on LLMs to infer the next action or waypoint. Among them, STMR [15] introduces a Semantic-Topo-Metric Representation that encodes current view, pose, and subgoal cues into matrix-form prompts for spatial reasoning over landmarks and directions. CityNavAgent [16] further enhances grounding via symbolic 2D landmark maps derived from real aerial imagery and spatial detection. In contrast, learning-based models directly align visual observations with language through end-to-end training. AeiralVLN [7] proposed the Look-ahead Guidance (LAG) strategy to improve CMA. Grid-based VS [18] reformulates aerial VLN as a grid-based view selection problem with coupled vertical-horizontal action modeling, bird’s-eye history fusion, and cross-modal alignment. More related to ours method, OpenFly [11] introduces keyframe-aware VLN and adaptive token merging to better handle long-horizon trajectories.

B. Vision-and-Language Navigation

Vision-and-language navigation (VLN) tasks require an agent to follow natural language instructions using visual observations to achieve a target location [26]. Early VLN benchmarks formulated navigation on a predefined graph of panoramic viewpoints, where the agent selects discrete actions to move between connected nodes [27], [28]. To move beyond the discrete setting, VLN-CE [29] replaced the navigation graph with free movement in simulation, where the agent executes mid-level actions, such as moving forward and turning. A variety of learning-based methods have been proposed under this setting, including cross-modal attention [30], memory-augmented agents [31], and planning-based approaches [32], [33]. A growing line of work has focused on training vision-language models that directly map RGB observations and instructions to navigation actions. NaVid [34] demonstrates that a vision-language model trained on large-scale continuous trajectories can effectively use monocular RGB video to model temporal context and predict actions, achieving strong performance. NaVILA [35] introduces a two-stage framework that maps visual observations and instructions into mid-level language actions, which are then executed by a learned locomotion policy, enabling instruction-conditioned control in low-level continuous environments. MonoDream [36] introduces auxiliary representation learning tasks that train a monocular agent to align visual semantics and action intent by predicting latent panoramic features. Uni-NaVid [37] unifies diverse navigation tasks within a single end-to-end framework by learning from multi-task RGB video data. VLN-R1 [38] combines supervised and reinforcement fine-tuning to enhance temporal reasoning and multi-step action planning.

While these approaches have made substantial progress, they are primarily developed for ground-based agents and

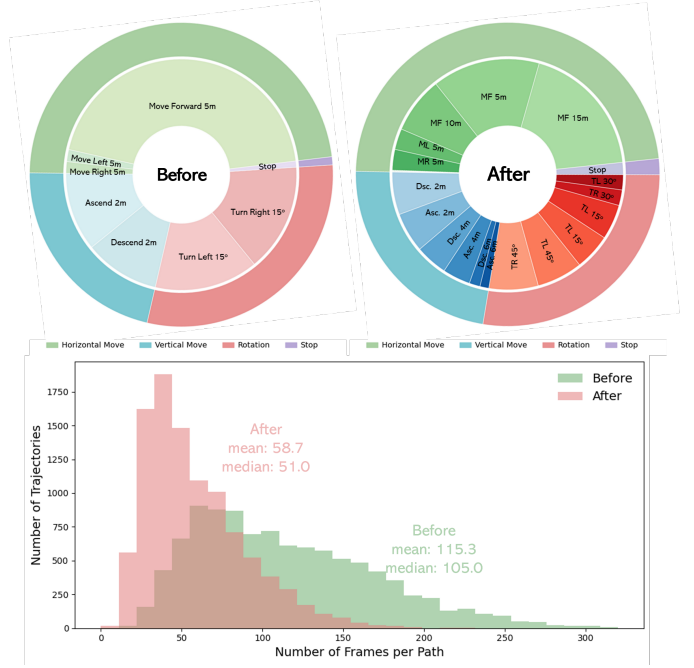


Fig. 2. Trajectory statistics before and after data preprocessing, showing that action merging and keyframe selection yield a richer action space and more compact navigation sequences. For brevity, we use MF for *move forward* etc.

remain limited in capturing the challenges inherent to aerial-based navigation, such as viewpoint variability, long-range flight paths, and complex 3D outdoor scenes.

III. METHOD

A. Problem Formulation

Aerial vision-and-language navigation. An aerial agent is provided with a natural language instruction $I = \{w_1, w_2, \dots, w_{N_I}\}$ describing the desired flight route in a continuous 3D environment. At time step t , the agent receives an observation $\tau_t = \{x_1, \dots, x_t\}$, consisting of first-person RGB images captured by the UAV’s onboard camera. Conditioned on visual observation τ_t and the instruction I , the agent selects an action a_t from the discrete action set $\mathcal{A} = \{\text{move forward}, \text{turn left}, \text{turn right}, \text{ascend}, \text{descend}, \text{move left}, \text{move right}, \text{stop}\}$. In AerialVLN-S environment, horizontal motions displace the agent by 5 units, vertical motions by 2 units, and turning applies a fixed 15° change in orientation. Executing a_t moves the agent to the next state in the environment, yielding the subsequent observation X_{t+1} . The objective is to generate an action sequence that guides the aerial agent to the location indicated by the instruction. An episode terminates when the agent chooses the *Stop* action or reaches the maximum step limit. Following AerialVLN protocol, a trajectory is deemed successful if the agent’s final position lies within 20 meters of the ground-truth destination.

B. Data Preprocessing

In data preprocessing stage, we refine the raw drone trajectories by applying action merging and keyframe selection, two complementary steps that improve the temporal structure

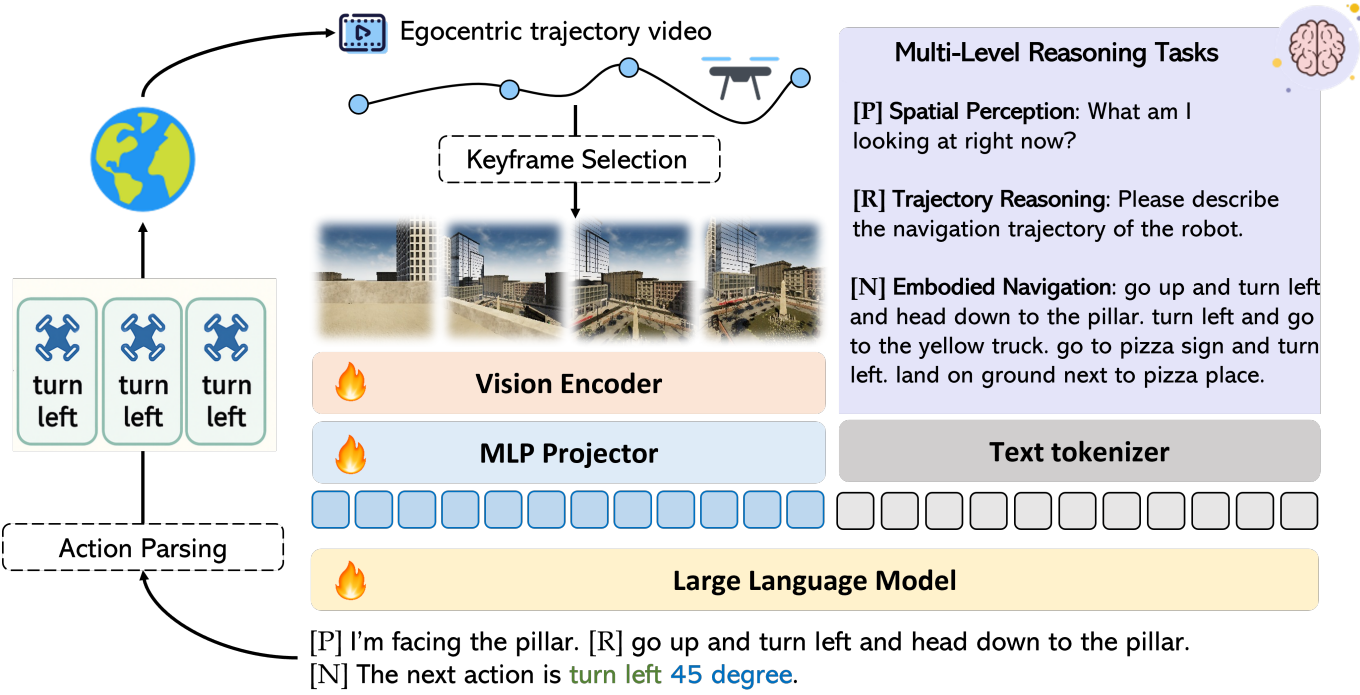


Fig. 3. Overview of our framework. Given egocentric keyframes selected from the onboard video stream, our model first encodes the visual observations through a vision encoder and a MLP projector to obtain visual tokens, while language instructions are processed by a text tokenizer. The unified multimodal tokens are then fed into a large language model that is jointly trained on three complementary tasks: (i) Spatial Perception, which queries the current scene; (ii) Trajectory Reasoning, which summarizes historical motion and infers the agent's navigational context; and (iii) Embodied Navigation, which predicts high-level action commands. The predicted textual action is further parsed and decomposed into a sequence of predefined motion primitives for execution in the physical environment.

of training samples. Together, these preprocessing steps organize trajectories into clearer motion segments paired with representative visual cues, improving the quality of supervision for navigation learning. As shown in Fig. 2, our approach expands the action vocabulary, produces a more balanced action distribution, and significantly shortens trajectories by eliminating redundant micro-actions.

Action Merging. UAV navigation trajectories are typically long and dominated by frequent forward micro-steps, leading to highly imbalanced and fragmented action sequences. To reduce fragmented micro-actions and enhance the semantic clarity of motion patterns, we merge consecutive identical actions into a single segment with a bounded length (e.g., combining three turn left 15° steps into a single turn left 45° step). This produces more meaningful action units and yields a more balanced and diverse action distribution.

Keyframe Selection. To further suppress temporal visual redundancy, we extract keyframes at the boundaries of the merged action segments. This simple yet effective strategy is motivated by the observation that abrupt changes in the agent’s motion—such as transitioning from straight movement to a turning action—are often caused by the appearance of landmarks. These turning points naturally delimit semantically meaningful transitions in the underlying trajectory. By selecting the frames at these boundaries as keyframes, we obtain a compact set of observations that preserves landmarks and other salient visual cues while filtering out redundant intermediate views. This yields a more informative and temporally

structured visual stream for downstream navigation learning.

C. Framework Overview

As illustrated in Fig. 3, our framework tackles the aerial vision-and-language navigation task by processing natural-language instructions together with an egocentric video stream under a unified next-token prediction paradigm.

Overall Pipeline. At each timestep, we sample a compact set of keyframes from the observation trajectory so far and pair them with the instruction. The keyframes are encoded into visual tokens through a vision encoder and projected into the language embedding space, while the instruction is tokenized independently. The resulting multimodal token sequence is fed into a large language model (LLM), which produces the next action directly in text form through autoregressive decoding. This action text is parsed into a predefined action set of low-level control commands and executed to update the drone’s state in 3D aerial environments. To strengthen the agent’s spatial understanding and its ability to interpret navigational progress, we introduce two auxiliary tasks, termed spatial perception and trajectory reasoning. The spatial perception task guides the agent to answer egocentric questions about the current scene, whereas the trajectory reasoning task requires summarizing the observation trajectory. Together, these tasks provide complementary supervision that refines the model’s representation of spatial structure and navigation dynamics, ultimately boosting aerial navigation performance.

Observation Encoding and Multimodal Tokenization. At each timestep t , the agent receives the current egocentric image x_t together with the accumulated visual trajectory. To obtain a compact yet informative representation, we uniformly sample K frames while always retaining the first frame and the current frame. The first frame provides a stable reference of the starting viewpoint, whereas the current frame serves as the primary basis for predicting the next navigation action; the remaining historical frames supply contextual cues for interpreting navigation progress. Let the sampled keyframes be $\mathcal{X}_t = \{x_1, x_2, \dots, x_K\}$ with $x_{t_K} = x_t$. Each frame is encoded by a vision backbone into patch-level features:

$$E_{t_i}^{\text{vis}} = \text{Enc}_{\text{vis}}(x_{t_i}) \in \mathbb{R}^{N \times C}. \quad (1)$$

Long-horizon trajectories may yield prohibitively long visual token sequences. To mitigate this, we apply a Spatial Token Compression (STC) module that aggregates non-overlapping $g \times g$ neighborhoods. A lightweight MLP projector aligns visual features to the LLM embedding space.

$$\begin{aligned} \tilde{E}_{t_i}^{\text{vis}} &= \text{STC}(E_{t_i}^{\text{vis}}) \in \mathbb{R}^{(N/g^2) \times (Cg^2)}, \\ Z_{t_i}^{\text{vis}} &= \text{Proj}_{\text{mlp}}(\tilde{E}_{t_i}^{\text{vis}}) \in \mathbb{R}^{(N/g^2) \times D}. \end{aligned} \quad (2)$$

The navigation instruction $I = \{\omega_1, \dots, \omega_L\}$ is tokenized by the LLM tokenizer to obtain text token $Z^{\text{text}} \in \mathbb{R}^{L \times D}$. We then concatenate visual and textual tokens into a unified multimodal sequence:

$$S_t = [Z_0^{\text{vis}}, \dots, Z_{t_K}^{\text{vis}}, Z^{\text{text}}], \quad (3)$$

which serves as the observation representation for navigation. The sequence is fed into the LLM backbone and finally we get the hidden state:

$$H_t = \text{LLM}(S_t), \quad (4)$$

from which the next action a_t is autoregressively generated in linguistic form.

Unified Prompting Interface. Aerial VLN poses substantially higher demands on scene understanding and temporal reasoning due to the semantic complexity of outdoor 3D environments and the long-horizon navigation trajectories. Effective navigation requires the agent to interpret fine-grained spatial cues, maintain awareness of its progression along the trajectory, and ground language instructions to visual observations across a large spatial scale. To support the acquisition of these complementary reasoning abilities, we adopt a unified prompting interface that formulates all tasks within the same next-token prediction paradigm, without any modification to the underlying model architecture. As shown in Fig. 4, we instantiate three prompt-driven task formulations that expose different levels of navigation-relevant reasoning:

Spatial Perception, Trajectory Reasoning, and Embodied Navigation. Spatial perception prompts require the model to answer egocentric, scene-centric questions based on the current view (e.g., “What object appears on the right side of the image?”), thereby reinforcing fine-grained geometric and semantic grounding. Trajectory reasoning prompts ask the model to summarize the observed image sequence ,

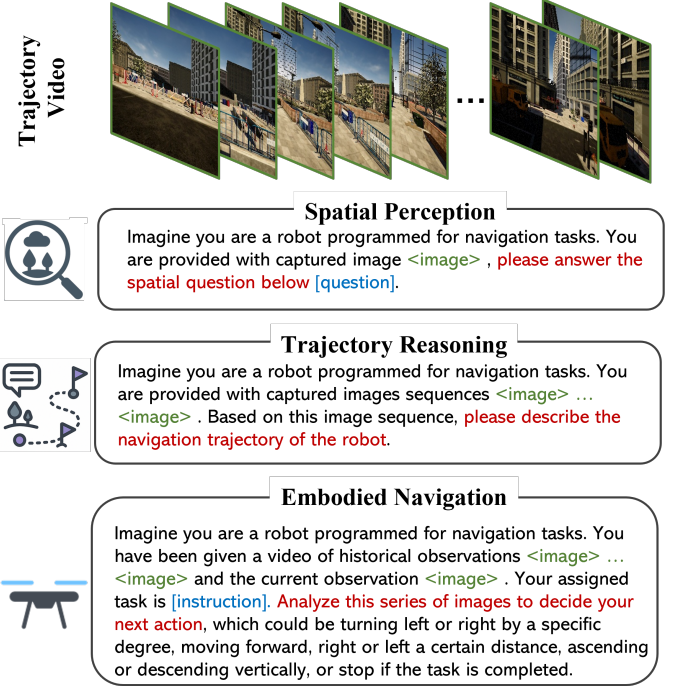


Fig. 4. Unified prompting interface for the proposed model. Through task-specific prompts, the model supports aerial navigation as the primary task, while also handling spatial perception and trajectory reasoning as auxiliary capabilities that enrich spatial understanding and temporal grounding.

encouraging structured understanding of navigation progress. Embodied navigation prompts instruct the model to predict the next control step in linguistic form, as we mentioned before. These task formulations provide complementary supervisory signals that strengthen the model’s multi-level reasoning over spatial structure and temporal trajectory evolution, thereby supporting more reliable navigation decision-making.

Action Parsing and Execution. Once the model outputs a textual action command (e.g., “The next action is move forward 15 units”), we apply a regular-expression parser to extract the action type and its numeric argument. The parsed action is then decomposed into low-level motion primitives (e.g., multiple fixed-step forward movements). These primitives are executed in an open-loop manner until all of them are completed, after which the agent receives the next visual observation from the environment, updates its trajectory history, and predicts the subsequent action.

D. Training Objective

Our model is trained in a multi-task setting that jointly supervises aerial navigation, spatial perception, and trajectory reasoning through autoregressive language modeling. Since navigation trajectories exhibit a highly imbalanced distribution of actions, we apply a frequency-based label reweighting strategy. Each action $a \in \mathcal{A}$ is assigned a normalized inverse-frequency weight,

$$w(a) = \sqrt{\frac{1/p(a)}{\frac{1}{|\mathcal{A}|} \sum_{b \in \mathcal{A}} 1/p(b)}}. \quad (5)$$

TABLE I
OVERVIEW OF THE CURATED DATASETS FOR MULTI-TASK TRAINING.

Task Type	Data Source	Description
Spatial Perception	Open3D-VQA (Sim env) + GQA (Real env)	Drone egocentric spatial reasoning + spatial-relation QA pairs
Trajectory Reasoning	AerialVLN (Sim env)	Sub-trajectory segmentation + progress summaries
Aerial Navigation	AerialVLN (Sim env)	Step-wise tuples (τ_t, I, a_t) after action merging and keyframe selection

The overall multi-task objective integrates supervision from all three tasks. Let \mathcal{B} denote the mixed training set. The loss is defined as

$$\mathcal{L} = \frac{1}{|\mathcal{B}|} \sum_{u \in \mathcal{B}} W(u) \ell_{\text{CE}}(y_u, z_u),$$

$$W(u) = \begin{cases} w(a_t), & u \in \mathcal{D}_{\text{nav}}, \\ \lambda_{\text{sp}}, & u \in \mathcal{D}_{\text{sp}}, \\ \lambda_{\text{tr}}, & u \in \mathcal{D}_{\text{tr}}, \end{cases} \quad (6)$$

$$\mathcal{B} = \mathcal{D}_{\text{nav}} \cup \mathcal{D}_{\text{sp}} \cup \mathcal{D}_{\text{tr}}.$$

where $W(u)$ denotes the task-specific weight assigned to sample u . The term $\ell_{\text{CE}}(y_u, z_u)$ is the standard autoregressive cross-entropy loss computed between ground truth y_u and model output z_u . For samples from other auxiliary tasks, we apply task-specific weighting to regulate their relative influence during optimization. λ_{sp} and λ_{tr} are the hyperparameters of weight for spatial perception and trajectory reasoning samples, respectively.

E. Implementation Details

Dataset Curation. To support the multi-task training objectives, we curate a mixed dataset that provides complementary supervision for action prediction, spatial grounding, and temporal reasoning, shown in Table I. Our curation is guided by two principles: maintaining a coherent input-output structure across tasks and constructing a balanced mixture that captures the diversity of aerial navigation scenarios. For aerial navigation task, we derive step-wise supervision from AerialVLN simulation trajectories by applying action merging and keyframe selection, producing compact training tuples (τ_t, I, a_t) . For spatial perception, we incorporate VQA-style supervision from the drone-centric subset of Open3D-VQA [14], complemented by a spatial-relation-focused subset of GQA [39] filtered for geometric predicates. To provide temporal abstraction signals, trajectory reasoning annotations are obtained by segmenting AerialVLN trajectories into ordered sub-trajectories and generating progress summaries aligned with instruction semantics. This curated mixture forms a coherent and comprehensive data blend for supervised fine-tuning of the proposed aerial VLN model.

Model Training. We fine-tune NVILA-lite-2B and NVILA-lite-8B on our aerial navigation task, initializing both models from their pretrained weights. Training is performed on 4 NVIDIA A100 GPUs using DeepSpeed ZeRO-3 optimization, with a learning rate of 2×10^{-5} . We employ a cosine decay schedule with a warm-up ratio of 0.03. We adopt a global

batch size of 128, achieved through a per-GPU batch size of 8 and 4 gradient accumulation steps. All models are trained for 1 epoch.

IV. EXPERIMENTS

A. Experimental Setup

Simulated environments. We conduct experiments on the AerialVLN-S benchmark [7], which provides a realistic aerial navigation setting rendered in AirSim and Unreal Engine 4. The dataset covers 17 compact outdoor scenes representing diverse urban environments such as residential areas, industrial zones, parks, and villages. For evaluation, the dataset allocates 12 environments to the training and validation-seen splits, while the validation-unseen split is drawn from 5 distinct scenes. Flight trajectories are collected by expert pilots, who follow naturalistic aerial routes to ensure realistic motion patterns and diverse path configurations. Overall, AerialVLN-S provides 10,113 language instructions for training, with 333 and 531 instructions assigned to the validation-seen and validation-unseen splits, respectively.

Evaluation Metrics. We adopt four standard metrics to evaluate aerial vision-and-language navigation [7]:

- **Navigation Error (NE/m).** Measuring goal-reaching accuracy by computing the Euclidean distance between the UAV's final position and the destination.
- **Success Rate (SR%).** Evaluating task completion as the proportion of episodes in which the UAV stops within a 20-meter radius of the destination.
- **Oracle Success Rate (OSR%).** Relaxing the success criterion by marking an episode successful if *any* point along the predicted trajectory falls within this 20-meter radius.
- **Success-weighted Dynamic Time Warping (SDTW%).** Assessing trajectory alignment by applying normalized DTW between the predicted and ground-truth paths and weighting the score by the Success Rate.

Baselines. We compare our approach against previous diverse baselines. These baselines fall into three categories [16]:

- **Statistical-based methods.** Random Sampling uniformly samples actions from the action space while Action Sampling selects actions according to the training-set action distribution.
- **Zero-shot LLM-based methods.** MapGPT [41] introduces a language-based online map representation to equip GPT-4v [42] with global spatial understanding, enabling adaptive multi-step planning for indoor VLN in a zero-shot setting. STMR [15] enhances spatial reasoning by introducing a Semantic–Topo–Metric Representation that allows LLMs to infer navigation decisions directly from structured scene

TABLE II

COMPARISON OF DIFFERENT METHODS ON THE AERIALVNL-S DATASET. OBSERVATIONS INCLUDE SINGLE RGB (S.RGB), DEPTH (DEPTH), PANORAMIC VIEW (PANO.), AND ODOMETRY INFORMATION (ODO.)

Method	Observation				Validation Seen				Validation Unseen			
	S.RGB	Depth	Pano.	Odo.	NE↓	SR↑	OSR↑	SDTW↑	NE↓	SR↑	OSR↑	SDTW↑
Grid-based VS [18]			✓	✓	70.3	20.8	33.4	10.2	121.3	7.4	16.1	2.5
CityNavAgent [16]		✓	✓	✓	80.8	13.9	30.2	5.1	60.2	11.7	35.2	5.0
Random Sampling					109.6	0.0	0.0	0.0	149.7	0.0	0.0	0.0
Action Sampling					213.8	0.9	5.7	0.3	237.6	0.2	1.1	0.1
LingUNet [40]	✓	✓			383.8	0.6	6.9	0.2	368.4	0.4	3.6	0.9
Seq2Seq [17]	✓	✓			146.0	4.8	19.8	1.6	218.9	2.3	11.7	0.7
CMA [17]	✓	✓			121.0	3.0	23.2	0.6	172.1	3.2	16.0	1.1
LAG [7]	✓	✓			90.2	7.2	15.7	2.4	127.9	5.1	10.5	1.4
SMTR [15]	✓	✓			96.3	12.6	<u>31.6</u>	<u>2.7</u>	119.5	10.8	<u>23.0</u>	<u>1.9</u>
MapGPT [41]	✓				124.9	2.1	4.7	0.8	107.0	0.0	0.0	0.0
NaVid [11]	✓				105.1	6.8	15.5	1.1	106.9	6.1	12.3	0.7
Openfly [34]	✓				127.2	8.1	21.8	1.6	113.8	7.6	18.2	1.5
Ours	✓				79.6	<u>11.4</u>	37.7	6.3	95.8	<u>8.1</u>	28.9	2.2

information. CityNavAgent [16] performs hierarchical semantic planning to predict waypoints in a zero-shot manner, supported by a global memory module that records past trajectories for improved long-horizon navigation.

- **Learning-based methods.** Seq2Seq [17] predicts actions using a recurrent policy that encodes visual observations and language instructions into a unified hidden representation. CMA [17] introduces cross-modal attention to better fuse RGB, depth, and textual cues for action prediction. LAG [7] adds a look-ahead guidance module. NaVid [34] is a video-based vision–language model that has demonstrated strong performance in indoor VLN. OpenFly [11] adopts a keyframe-aware VLN architecture and uses adaptive token sampling over historical observations.

B. Results on AerialVNL-S Benchmark

1) *Quantitative Results:* To ensure a fair comparison, we categorize methods by their sensor configurations, distinguishing RGB-only agents from those that rely on panoramic inputs, depth sensing, or odometry. Within the RGB-only group, our method achieves strong performance on all metrics and attains the best overall results, with comparable to SMTR [15], which required external depth information. The proposed method is also competitive with panoramic baselines, especially in SDTW. This is particularly meaningful on AerialVNL setting, where many trajectories contain turn-backs and repeated segments, making SDTW a more informative measure of instruction following than SR alone. Panoramic methods typically require multiple cameras or repeated in-place rotations to build 360° observations, which increases time and energy costs for UAVs, whereas our model operates from a single-view RGB stream and thus better matches realistic deployment constraints. MapGPT [41] and NaVid [34], which are strong indoor VLN baseline, perform notably worse in outdoor aerial setting, underscoring the additional challenges posed by large-scale, sparsely structured environments. Compared with the

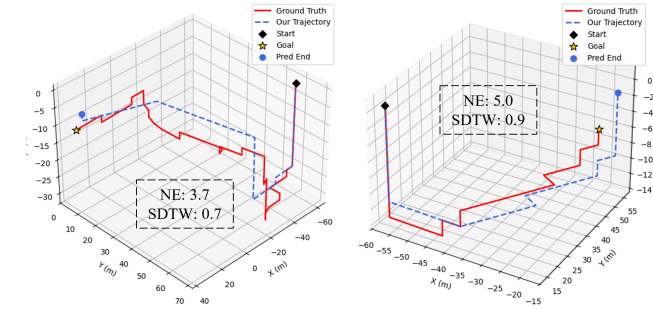


Fig. 5. Qualitative comparison between predicted and ground-truth drone trajectories in 3D space. Across multiple validation episodes, the predicted paths follow the global route structure, capturing major turns, long-range transitions, and altitude changes required by language instruction. These results highlight strong 3D spatial reasoning and stable flight control from egocentric observations.

most related OpenFly [11] framework, our approach further benefits from long-horizon history modeling and auxiliary tasks, leading to more stable long-range behavior. Overall, these results establish a new state of the art for monocular RGB-only aerial VLN and validate the effectiveness of our unified framework for spatial, temporal, and embodied reasoning. Fig. 5 compares the predicted 3D flight paths with the reference routes. The predicted trajectories preserve the overall geometric structure of the routes, including the major turning segments, long-range direction changes, and the characteristic height variations implied by the instruction. Although small local deviations occasionally appear, the agent often recovers from these offsets and continues to produce geometrically coherent paths over extended horizons. The trajectories also converge toward the intended final region, reflecting stable motion patterns derived solely from egocentric RGB observations in large-scale outdoor environments.

Instruction: take off after *rising* to the height slightly higher. *proceed forward* and *dive down* by facing the *wood tent*. *turn right fly above* by crossing the *blue cover hut*. *fly forward* to the *wooden house*. *dive down land* by facing the *bottom of the above mentioned house*.



Instruction: *going through the shops* and *passing the small lifter*. *rotating by the bike parking* and *going up*. *going through the train station* and *going toward the beige building*. *rotating by the green shop* and *going to the left*. *passing through the train station*. *turning back* through the *train station* and *going toward the white building*. *landing* by the *white and black building*.



Fig. 6. Visualizations of our method on AerialVNL-S benchmark. Our model successfully follows detailed long-horizon instructions, grounds visual landmarks, and executes correct spatial maneuvers across complex outdoor scenes, demonstrating strong instruction-following consistency and robust navigation ability. For clarity, colored elements denote **landmarks** and **action phrases**. Trajectories are visually grouped to facilitate analysis of long-horizon behaviors.

2) *Qualitative Analysis:* We provide qualitative navigation trajectories in Fig. 6 to assess the model’s ability to interpret and ground natural language instructions in realistic outdoor environments. The first example illustrates a medium-length instruction including several landmark-based references. Our agent demonstrates reliable instruction-following behavior by consistently grounding entities such as *shops*, *bike parking*, and *green shop*, and by executing the corresponding spatial maneuvers (e.g., *turning*, *approaching*, *passing*) at the appropriate visual cues. This indicates that the model preserves strong cross-modal alignment between linguistic expressions and visual observations, a fundamental capability for step-by-step decision-making in VLN. The second example showcases navigation under a significantly longer and more descriptive instruction spanning over one hundred actions. Throughout this extended trajectory, the agent maintains instruction consistency, preserves stable temporal grounding, and generates coherent movement decisions despite the increased complexity. These results highlight the robustness of our model in long-horizon instruction following, a key requirement for practical UAV VLN in unconstrained outdoor environments. To analyze the trajectory behavior of our navigation policy,

Fig. 7 presents qualitative examples from the auxiliary VQA datasets used in training. On Open3D-VQA dataset, the model correctly answers 3D spatial queries such as which object is higher or what lies to the left/right in an egocentric aerial view. On the GQA subset, it identifies objects and resolves simple spatial relations in visually cluttered scenes. These

examples show that the model can interpret scene geometry and spatial layout from egocentric inputs. Fig. 8 presents qualitative examples from the trajectory reasoning task. Given the historical egocentric visual trajectory, the model produces a concise natural-language description that captures the high-level motion pattern and the principal scene transitions along the route. The generated summaries demonstrate consistent temporal abstraction by identifying turning segments, periods of forward movement, and transitions associated with spatial landmarks such as parks, intersections, and surrounding buildings. Moreover, the model reflects the causal structure of the trajectory by linking sequences of actions to the corresponding visual and semantic changes in the environment. These examples show that the model can integrate long-term dependencies and organize extended action sequences into coherent semantic units, which provides a complementary form of temporal grounding beyond low-level action prediction.

C. Ablation Study

1) *Effect of Auxiliary Tasks:* We conduct ablation experiments to evaluate the effect of the two auxiliary tasks: Spatial Prediction (SP) and Trajectory Reasoning (TR). Without auxiliary supervision, the policy shows limited spatial grounding and produces the lowest SR and SDTW on both splits. SP leads to consistent gains, confirming that geometric cues improve local action grounding. Incorporating TR further boosts performance, with the largest improvements on unseen environments, where long-horizon cues are critical for handling novel

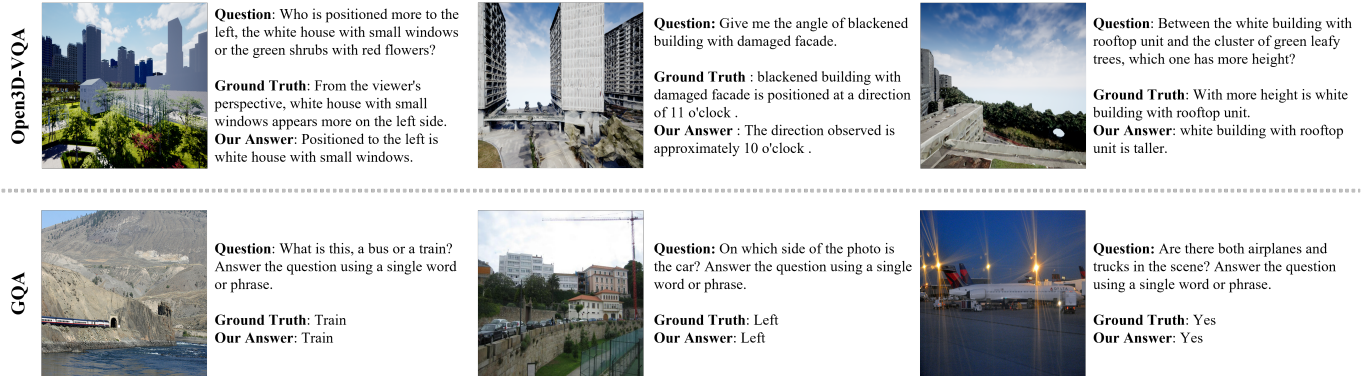


Fig. 7. Qualitative results on auxiliary VQA tasks. Top: examples from the Open3D-VQA dataset [14], where the model answers 3D spatial queries including relative relations and geometric orientation. Bottom: examples from GQA [39], covering object grounding and relational reasoning. These examples illustrate the model's of spatial understanding and positional reasoning, which is crucial for language-guided UAV navigation.



Ground Truth: *lift off* and *turn left* facing the *building* touching the *pipe* and *head straight*, before the *aluminum walkway* on the *roof* *turn left* facing left of the *open garage*.

Our Answer: *After taking off*, the drone *turns left* toward the *building* with the *pipe*, *proceeds straight*, and then *turns left* again just before the *aluminum roof walkway*, aligning with the *open garage*.

Fig. 8. Qualitative results on trajectory summary task. The model summarizes the route by identifying key landmarks (building, pipe, walkway, garage) and the major motion segments (take-off, left turns, forward movement), demonstrating temporal understanding of the visual trajectory.

TABLE III

ABALATION STUDY ON AUXILIARY TASKS: SPATIAL PREDICTION (SP) AND TRAJECTORY REASONING (TR). BOTH TASKS IMPROVE SUCCESS RATE (SR) AND TRAJECTORY QUALITY (SDTW) ON BOTH SEEN AND UNSEEN ENVIRONMENTS.

Auxiliary Tasks	Val Seen		Val Unseen	
	SP	TR	SR \uparrow	SDTW \uparrow
			9.6	4.5
✓			10.8	5.4
✓	✓		11.4	6.3
			8.1	2.2

layouts. These results demonstrate that the two objectives are complementary: SP enhances local spatial understanding, while TR strengthens temporal reasoning. Their combination yields a more reliable navigation policy and supports the design of our multi-task framework, reinforcing our goal of unifying spatial, temporal, and embodied reasoning within a single model.

TABLE IV

COMPARISON OF DIFFERENT HISTORY REPRESENTATION STRATEGIES ON AERIALVNL-S VAL-UNSEEN SPLIT.

History Strategy	SR \uparrow	SDTW \uparrow
Current-Only (2B)	4.1	1.1
Short-Term Memory Bank (2B, $k = 8$)	4.3	1.2
Long-Horizon Uniform Sampling (2B, $k = 8$)	5.5	1.6
Long-Horizon Uniform Sampling (8B, $k = 8$)	5.9	1.6

2) *Effect of History Representation Strategies:* We compare three history representation strategies. (1) *Current-Only*, where the model relies solely on the latest observation, often leading to unstable behaviors such as repeated fine-grained heading corrections. (2) *Short-Term Memory Bank*, which maintains a fixed-size memory bank following a first-in-first-out (FIFO) policy, keeping only the most recent observations and discarding earlier ones [11]. This provides short-range temporal cues while discards earlier information essential for global naviga-

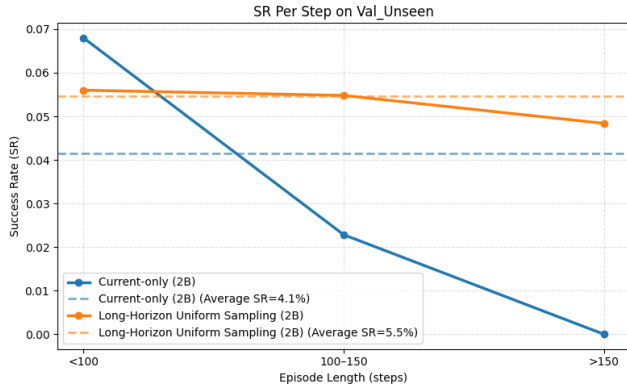


Fig. 9. Success rate across different trajectory lengths on the Val-Unseen split. Long-Horizon Uniform Sampling maintains stable performance across episodes of varying lengths.

tion. (3) *Long-Horizon Uniform Sampling*, which uniformly samples a small set of frames from the entire past trajectory to provide long-range visual context. Table IV compares these history representation strategies. Among them, Long-Horizon Uniform Sampling ($k = 8$) achieves the best overall performance. By drawing observations uniformly from entire past trajectory, this strategy preserves both short-term motion cues and long-range scene information. As a result, it provides a more reliable temporal context than relying solely on the current frame or restricting history to a short FIFO queue. We compare these strategies using the NVILA-2B model for computational efficiency. The larger 8B variant follows the same trend and achieves consistently higher accuracy.

To further analyze how different history strategies behave under varying temporal horizons, we group the Val-Unseen episodes into three categories based on their trajectory length and report the per-step success rate for each method in Fig. 9. The Current-Only baseline performs reasonably well on short trajectories because the goal is often visible early, but its accuracy declines sharply as the trajectory becomes longer, indicating limited robustness without historical context. The Long-Horizon Uniform Sampling strategy maintains higher performance across all trajectory lengths, with clear advantages on medium and long episodes where global scene information becomes crucial. These results highlight the importance of accessing long-range temporal cues for stable navigation in large, visually diverse environments.

3) *Effect of Action Merging, Keyframe Selection and Label Reweighting*: Table V reports the effect of action merging (AM), keyframe selection (KS), and label reweighting (LR). For computational efficiency, this ablation uses the NVILA-2B model without auxiliary tasks, and all variants adopt a long-horizon uniform sampling of 8 history frames. Enabling action merging leads to immediate gains, as consolidating micro-actions into coherent motion segments produces cleaner supervisory signals compared to raw fragmented steps. Excessively large merge lengths slightly degrade performance, likely because they skip important visual cues and reduce the model’s ability to adapt to local changes. We therefore set the maximum merge length to 3. Adding keyframe selection

TABLE V

ABLATION STUDY ON THE EFFECT OF ACTION MERGING (AM), KEYFRAME SELECTION (KS) AND LABEL REWEIGHTING (LR) ON AERIALVLN-S VAL-SEEN SPLIT. ALL OF THEM CONSISTENTLY IMPROVE PERFORMANCE ACROSS ALL METRICS.

AM	KS	LR	NE↓	SR↑	OSR↑	SDTW↑
			90.2	1.8	20.5	0.7
✓			91.5	3.0	26.8	1.4
✓	✓		87.1	5.7	28.9	1.9
✓	✓	✓	82.1	8.1	32.2	3.8

further improves navigation accuracy. Selecting the boundaries of merged actions as keyframes provides a more structured trajectory history in which visual transitions align with meaningful motion changes. This reduces temporal redundancy while preserving observations most relevant to spatial landmarks. Finally, incorporating label reweighting achieves the best overall performance. By balancing the contribution of long merged segments and short corrective actions, it prevents the model from overfitting to frequent but low-impact motions and strengthens action-level supervision. Overall, the combined use of AM, KS, and LR yields substantial improvements in SR and SDTW, demonstrating that structuring the action sequence and rebalancing its supervision are both crucial for reliable aerial navigation.

D. Failure Case Analysis

Although our method achieves strong performance and outperforms competitive baselines, it is still susceptible to several typical failure modes. To better understand the remaining challenges and guide future improvements, we further analyze its most common failure cases below. A common failure mode arises from ambiguous instructions that provide only a sequence of low-level actions without any accompanying landmark references (e.g., “rotate, go straight, turn left, turn right, hold on”). Such instructions lack grounding anchors that would normally guide the agent in determining where a directional change or stop should occur. Under this setting, the agent receives no observable cues to align the action sequence with the environment, making it difficult to infer the intended spatial context. Another failure mode arises from the intrinsic limitations of single-view RGB perception in complex outdoor environments. When the agent lacks sufficient observational coverage, such as when critical cues briefly appear at the edge of view, the model may fail to terminate at the correct moment or overshoot the intended point, resulting in unnecessary backtracking or redundant movement. This behavior reflects the inherent difficulty of aligning long-horizon instructions with first-person observations. Enhancing viewpoint robustness, increasing the diversity of training trajectories, or exposing the model to more error-recovery scenarios in simulation could help mitigate such issues.

V. CONCLUSION

In this paper, we present a unified framework for aerial vision-and-language navigation that operates solely on monocular

ular egocentric RGB inputs and natural language instructions, eliminating the need for panoramic observations, depth sensing, or external localization modules. To address core challenges posed by the complexity of large-scale outdoor scenes and the long-horizon nature of aerial navigation, we reformulate aerial VLN as a next-token prediction problem and integrates spatial perception, trajectory reasoning, and action generation through task-specific prompts. Experiments on the Aerial VLN benchmark demonstrate that our method achieves new state-of-the-art performance among RGB-only approaches and significantly narrows the gap with panoramic RGB-D counterparts. This work highlights the potential of scalable, prompt-driven multimodal learning as an efficient solution for deploying embodied aerial agents in real-world scenarios.

REFERENCES

- [1] A. Khan, S. Gupta, and S. K. Gupta, “Emerging uav technology for disaster detection, mitigation, response, and preparedness,” *Journal of Field Robotics*, vol. 39, no. 6, pp. 905–955, 2022.
- [2] H. Yao and X. Liang, “Autonomous exploration under canopy for forest investigation using lidar and quadrotor,” *IEEE Transactions on Geoscience and Remote Sensing*, vol. 62, pp. 1–19, 2024.
- [3] Y. Xi, W. Jia, Q. Miao, J. Feng, J. Ren, and H. Luo, “Detection-driven exposure-correction network for nighttime drone-view object detection,” *IEEE Transactions on Geoscience and Remote Sensing*, vol. 62, pp. 1–14, 2024.
- [4] X. Wu, L. Wang, J. Guan, H. Ji, L. Xu, Y. Hou, and A. Fei, “Dhanet: Dual-stream hierarchical interaction networks for multimodal drone object detection,” *IEEE Transactions on Geoscience and Remote Sensing*, 2025.
- [5] Y. Yuan, Y. Wu, L. Zhao, Y. Liu, and Y. Pang, “Tlsh-mot: Drone-view video multiple object tracking via transformer-based locally sensitive hash,” *IEEE Transactions on Geoscience and Remote Sensing*, 2025.
- [6] Y. Xiao, J. Wang, Z. Zhao, B. Jiang, C. Li, and J. Tang, “Uav video vehicle detection: Benchmark and baseline,” *IEEE Transactions on Geoscience and Remote Sensing*, 2025.
- [7] S. Liu, H. Zhang, Y. Qi, P. Wang, Y. Zhang, and Q. Wu, “Aerialvlvn: Vision-and-language navigation for uav,” in *Proceedings of the IEEE/CVF International Conference on Computer Vision*, 2023, pp. 15 384–15 394.
- [8] Y. Fan, W. Chen, T. Jiang, C. Zhou, Y. Zhang, and X. Wang, “Aerial vision-and-dialog navigation,” in *Findings of the Association for Computational Linguistics: ACL 2023*, 2023, pp. 3043–3061.
- [9] J. Lee, T. Miyanishi, S. Kurita, K. Sakamoto, D. Azuma, Y. Matsuo, and N. Inoue, “Citynav: A large-scale dataset for real-world aerial navigation,” in *Proceedings of the IEEE/CVF International Conference on Computer Vision*, 2025, pp. 5912–5922.
- [10] X. Wang, D. Yang, Z. Wang, H. Kwan, J. Chen, W. Wu, H. Li, Y. Liao, and S. Liu, “Towards realistic uav vision-language navigation: Platform, benchmark, and methodology,” in *The Thirteenth International Conference on Learning Representations*.
- [11] Y. Gao, C. Li, Z. You, J. Liu, Z. Li, P. Chen, Q. Chen, Z. Tang, L. Wang, P. Yang *et al.*, “Openfly: A versatile toolchain and large-scale benchmark for aerial vision-language navigation,” *arXiv e-prints*, pp. arXiv:2502, 2025.
- [12] R. Wu, Y. Zhang, J. Chen, L. Huang, S. Zhang, X. Zhou, L. Wang, and S. Liu, “Aeroduо: Aerial duo for uav-based vision and language navigation,” in *Proceedings of the 33rd ACM International Conference on Multimedia*, 2025, pp. 2576–2585.
- [13] Y. Zhao, K. Xu, Z. Zhu, Y. Hu, Z. Zheng, Y. Chen, Y. Ji, C. Gao, Y. Li, and J. Huang, “Cityeqa: A hierarchical llm agent on embodied question answering benchmark in city space,” *arXiv preprint arXiv:2502.12532*, 2025.
- [14] W. Zhang, Z. Zhou, Z. Zheng, C. Gao, J. Cui, Y. Li, X. Chen, and X.-P. Zhang, “Open3dqa: A benchmark for comprehensive spatial reasoning with multimodal large language model in open space,” *arXiv preprint arXiv:2503.11094*, 2025.
- [15] Y. Gao, Z. Wang, L. Jing, D. Wang, X. Li, and B. Zhao, “Aerial vision-and-language navigation via semantic-topo-metric representation guided llm reasoning,” *arXiv preprint arXiv:2410.08500*, 2024.
- [16] W. Zhang, C. Gao, S. Yu, R. Peng, B. Zhao, Q. Zhang, J. Cui, X. Chen, and Y. Li, “Citynavagent: Aerial vision-and-language navigation with hierarchical semantic planning and global memory,” *arXiv preprint arXiv:2505.05622*, 2025.
- [17] J. Krantz, E. Wijmans, A. Majumdar, D. Batra, and S. Lee, “Beyond the nav-graph: Vision-and-language navigation in continuous environments,” in *European Conference on Computer Vision*. Springer, 2020, pp. 104–120.
- [18] G. Zhao, G. Li, J. Pan, and Y. Yu, “Aerial vision-and-language navigation with grid-based view selection and map construction,” *arXiv preprint arXiv:2503.11091*, 2025.
- [19] B. Lindqvist, S. S. Mansouri, J. Haluška, and G. Nikolakopoulos, “Reactive navigation of an unmanned aerial vehicle with perception-based obstacle avoidance constraints,” *IEEE Transactions on Control Systems Technology*, vol. 30, no. 5, pp. 1847–1862, 2021.
- [20] Y. Zhang, Y. Hu, Y. Song, D. Zou, and W. Lin, “Learning vision-based agile flight via differentiable physics,” *Nature Machine Intelligence*, pp. 1–13, 2025.
- [21] S. Wang, F. Jiang, B. Zhang, R. Ma, and Q. Hao, “Development of uav-based target tracking and recognition systems,” *IEEE Transactions on Intelligent Transportation Systems*, vol. 21, no. 8, pp. 3409–3422, 2019.
- [22] A. V. Savkin, W. Ni, and M. Eskandari, “Effective uav navigation for cellular-assisted radio sensing, imaging, and tracking,” *IEEE Transactions on Vehicular Technology*, vol. 72, no. 10, pp. 13 729–13 733, 2023.
- [23] Y. Liu, Z. Ma, Y. Yang, M. Wang, and Y. Niu, “A framework for visual target navigation for quadcopter based on large language models in unknown environment,” in *International Conference on Cognitive Computation and Systems*. Springer, 2024, pp. 99–110.
- [24] W. Zhang, Y. Liu, X. Wang, X. Chen, C. Gao, and X. Chen, “Demo abstract: Embodied aerial agent for city-level visual language navigation using large language model,” in *2024 23rd ACM/IEEE International Conference on Information Processing in Sensor Networks (IPSN)*. IEEE, 2024, pp. 265–266.
- [25] L. Yumeng, W. Tao, and Q. Tony, “Empowering uavs with large models: Prospects and challenges,” p. 103860, 2025.
- [26] W. Wu, T. Chang, X. Li, Q. Yin, and Y. Hu, “Vision-language navigation: a survey and taxonomy,” *Neural Computing and Applications*, vol. 36, no. 7, pp. 3291–3316, 2024.
- [27] P. Anderson, Q. Wu, D. Teney, J. Bruce, M. Johnson, N. Sünderhauf, I. Reid, S. Gould, and A. Van Den Hengel, “Vision-and-language navigation: Interpreting visually-grounded navigation instructions in real environments,” in *Proceedings of the IEEE conference on computer vision and pattern recognition*, 2018, pp. 3674–3683.
- [28] A. Ku, P. Anderson, R. Patel, E. Ie, and J. Baldwin, “Room-across-room: Multilingual vision-and-language navigation with dense spatiotemporal grounding,” in *Proceedings of the 2020 Conference on Empirical Methods in Natural Language Processing (EMNLP)*, 2020, pp. 4392–4412.
- [29] J. Krantz, E. Wijmans, A. Majumdar, D. Batra, and S. Lee, “Beyond the nav-graph: Vision-and-language navigation in continuous environments,” in *European Conference on Computer Vision*. Springer, 2020, pp. 104–120.
- [30] Y. Hong, Q. Wu, Y. Qi, C. Rodriguez-Opazo, and S. Gould, “Vln bert: A recurrent vision-and-language bert for navigation,” in *Proceedings of the IEEE/CVF conference on Computer Vision and Pattern Recognition*, 2021, pp. 1643–1653.
- [31] Z. Wang, X. Li, J. Yang, Y. Liu, and S. Jiang, “Gridmm: Grid memory map for vision-and-language navigation,” in *Proceedings of the IEEE/CVF International conference on computer vision*, 2023, pp. 15 625–15 636.
- [32] D. An, H. Wang, W. Wang, Z. Wang, Y. Huang, K. He, and L. Wang, “Etpnav: Evolving topological planning for vision-language navigation in continuous environments,” *IEEE Transactions on Pattern Analysis and Machine Intelligence*, 2024.
- [33] H. Wang, W. Liang, L. Van Gool, and W. Wang, “Dreamwalker: Mental planning for continuous vision-language navigation,” in *Proceedings of the IEEE/CVF international conference on computer vision*, 2023, pp. 10 873–10 883.
- [34] J. Zhang, K. Wang, R. Xu, G. Zhou, Y. Hong, X. Fang, Q. Wu, Z. Zhang, and H. Wang, “Navid: Video-based vlm plans the next step for vision-and-language navigation,” *arXiv preprint arXiv:2402.15852*, 2024.
- [35] A.-C. Cheng, Y. Ji, Z. Yang, Z. Gongye, X. Zou, J. Kautz, E. Biyik, H. Yin, S. Liu, and X. Wang, “Navila: Legged robot vision-language-action model for navigation,” in *RSS*, 2025.
- [36] S. Wang, Y. Wang, W. Li, Y. Wang, M. Chen, K. Wang, Z. Su, X. Cai, Y. Jin, D. Li *et al.*, “Monodream: Monocular vision-language navigation with panoramic dreaming,” *arXiv preprint arXiv:2508.02549*, 2025.

- [37] J. Zhang, K. Wang, S. Wang, M. Li, H. Liu, S. Wei, Z. Wang, Z. Zhang, and H. Wang, “Uni-navid: A video-based vision-language-action model for unifying embodied navigation tasks,” *arXiv preprint arXiv:2412.06224*, 2024.
- [38] Z. Qi, Z. Zhang, Y. Yu, J. Wang, and H. Zhao, “Vln-rl: Vision-language navigation via reinforcement fine-tuning,” *arXiv preprint arXiv:2506.17221*, 2025.
- [39] D. A. Hudson and C. D. Manning, “Gqa: A new dataset for real-world visual reasoning and compositional question answering,” in *Proceedings of the IEEE/CVF conference on computer vision and pattern recognition*, 2019, pp. 6700–6709.
- [40] D. Misra, A. Bennett, V. Blukis, E. Niklasson, M. Shatkhin, and Y. Artzi, “Mapping instructions to actions in 3d environments with visual goal prediction,” *arXiv preprint arXiv:1809.00786*, 2018.
- [41] J. Chen, B. Lin, R. Xu, Z. Chai, X. Liang, and K.-Y. K. Wong, “Mapgpt: Map-guided prompting with adaptive path planning for vision-and-language navigation,” in *Proceedings of the 62nd Annual Meeting of the Association for Computational Linguistics*, 2024.
- [42] J. Achiam, S. Adler, S. Agarwal, L. Ahmad, I. Akkaya, F. L. Aleman, D. Almeida, J. Altenschmidt, S. Altman, S. Anadkat *et al.*, “Gpt-4 technical report,” *arXiv preprint arXiv:2303.08774*, 2023.



Huilin Xu (Student Member, IEEE) received the B.E. degree with honors from the School of Information Science and Engineering, Fudan University, Shanghai, China, in 2021. She is currently pursuing a Ph.D. degree at the Key Laboratory of Information Science of Electromagnetic Waves (MoE), Fudan University. Her research interests focus on visual reasoning, vision-based reinforcement learning, and robotic learning.



Zhuoyang Liu (Student Member, IEEE) received the B.E. degree from Wuhan University, Wuhan, Hubei, China, in 2020. She is currently pursuing the Ph.D. degree in electromagnetic science with the Key Laboratory of Information Science of Electromagnetic Waves, Fudan University, Shanghai, China. Her research interests include signal processing, Dual-Function Radar-Communication systems, reconfigurable intelligence surfaces, and the combination of artificial intelligence and electromagnetic waves.



Yixiang Luomei (S'18-M'22) received the B.E. and M.E. in Electronic and Communication Engineering from Xidian University, Xi'an, China, and the Ph.D in Electronic Information Engineering from Fudan University, Shanghai, China, in 2014, 2018 and 2022, respectively. From 2022 to 2023, she was a Research Fellow with the National University of Singapore, Singapore. Since 2013, she has been a Research Assistant of the MoE Key Lab for Information Science of Electromagnetic Waves, School of Information Science and Technology, Fudan University, Shanghai, China. She has published more than 10 papers in peer-reviewed journals, among some conference papers and patents. She is currently working on intelligent processing of electromagnetic signals, UAV SAR imaging, and ISAC sensing.



Feng Xu (Member, IEEE) received the B.E. degree (Hons.) in information engineering from Southeast University, Nanjing, China, in 2003, and the Ph.D. degree (Hons.) in electronic engineering from Fudan University, Shanghai, China, in 2008. From 2008 to 2010, he was a Post-Doctoral Fellow with the National Oceanic and Atmospheric Administration (NOAA) Center for Satellite Applications and Research, Camp Springs, MD, USA. From 2010 to 2013, he worked with Intelligent Automation Inc., Rockville, MD, USA, and NASA Goddard Space Flight Center, Greenbelt, MD, USA, as a Research Scientist. In 2012, he was selected for China's Global Experts Recruitment Program and subsequently returned to Fudan University, in 2013, where he is currently a Professor and the Vice Dean of the School of Information Science and Technology and the Vice Director of the electromagnetic waves (MoE) Key Laboratory for Information Science of Electromagnetic Waves. His research interests include electromagnetic scattering modeling, SAR information retrieval, and radar system development.

Dr. Xu is a Topic Associate Editor of the IEEE TRANSACTIONS OF GEOSCIENCE AND REMOTE SENSING and was an Associate Editor of the IEEE GEOSCIENCE AND REMOTE SENSING LETTERS (2014–2021). He is the Founding Chair of the IEEE GRSS Shanghai Chapter and an IEEE GRSS AdCom Member.